doi.org/10.36721/PJPS.2025.38.5.REG.14346.1

Cantharidic acid inhibits the malignant progression of colorectal cancer by inhibiting aerobic glycolysis and regulating the PI3K/Akt/P53 pathway

Yan Wei[#1], Shulin Dai[#1], Dongyun Zhang[1], Ting Zhang[1], Xiaoyu Wang[2], Bolin Liu[3], Wei Huang[4], Yin Li[5] and Mingliao Niu[6]*

[1]College of Basic Medicine, Nanyang Medicial College, Nanyang, Henan Province, China
[2]College of Pharmacy, Nanyang Medicial College, Nanyang, Henan Province, China
[3]College of Life Science, Nanyang Normal University, Nanyang, Henan Province, China
[4]College of Traditional Chinese Medicine, Nanyang Medicial College, Nanyang, Henan Province, China
[5]The First Affiliated Hospital, Nanyang Medicial College, Nanyang, Henan Province, China
[6]Anorectal Zone II, Henan Provincial Hospital of Traditional Chinese Medicine (The Second Affiliated Hospital of Henan University of Chinese Medicine), Zhengzhou, Henan Province, China

Abstract: Cantharidic acid (CA) has shown effective anticancer activity against many solid tumor cells, but it has not been reported in colorectal cancer (CRC). The PFKFB3 overexpression vector was transfected into SW480 and HT29 cells and the cells were treated with CA and PI3K activator 740 Y-P for 24 h. The malignant progression of the cells was evaluated through CCK-8, EdU, Transwell, flow cytometry, LDH release assay and Hoechst 33258 fluorescence. The expressions of aerobic glycolysis (AEG) and PI3K/Akt/P53 pathway were detected using the kit, extracellular acidification rate (ECAR) assay and Western blot. The subcutaneous tumor model was established by subcutaneous injection of SW480 cells. CA could significantly reduce the proliferation, migration and invasion of SW480 and HT29 cells and promote apoptosis and trigger cell cycle arrest. CA could reduce glucose uptake, lactic acid production and glycolytic capacity, reduce p-PI3K and p-Akt protein levels, raise P53 protein level. PFKFB3 overexpressed promoted CRC malignant progression. 740 Y-P could increase the AEG of CRC cells. Finally, CA reduced the volume and weight of CRC xenografts in mice and inhibited AEG and malignant biological behavior. In conclusion, CA inhibited AEG and malignant progression of CRC cells by regulating the PI3K/Akt/P53 pathway.

Keywords: Cantharidic acid; aerobic glycolysis; colorectal cancer; PI3K/Akt/P53 pathway

Submitted on 19-03-2025 – Revised on 14-04-2025– Accepted on 07-07-2025

INTRODUCTION

Colorectal cancer (CRC) is the third largest cancer in the world and ranks second in the current cancer mortality rate (Abedizadeh *et al.*, 2024). CRC incidence and mortality are increasing. According to statistics, there are 517,100 new CRC patients in China in 2022, accounting for 10.7% of all malignant tumors and the incidence rate in men is significantly higher than that in women. The incidence of CRC tends to be younger and the mortality rate continues to increase (Yang and Liu, 2020). However, the current first-line treatment measures often have problems such as drug resistance of tumor cells and large adverse reactions. Therefore, it is vital to investigate new and more effective therapeutic drugs and targets for the treatment and prognosis of CRC (Bausys *et al.*, 2022).

Most tumor cells provide energy for themselves through aerobic glycolysis (AEG) without the participation of oxygen and mitochondria. The AEG pathway is a special effect of tumor cells to obtain energy through glucose uptake and lactic acid production (Fukushi *et al.*, 2022). Glucose is metabolized by AEG and AEG undergoes a multi-stage reaction step to finally obtain pyruvate. The uptake of glucose by cancer cells is significantly increased and the resulting pyruvate leaves mitochondria and is converted into lactic acid by lactate dehydrogenase (LDH). AEG can rapidly produce adenosine triphosphate (ATP) and provide energy for the growth and metastasis of tumor cells (Icard *et al.*, 2018). Studies have found that high level of POU domain class 2 transcription factor 1 (POU2F1) can promote the growth of colon cancer cells, AEG and the pentose phosphate pathway (Lin *et al.*, 2022). This metabolic change of CRC cells sometimes occurs before the mutation or inactivation of cancer genes, which in turn leads to the enhancement of AEG metabolism. These metabolic changes will affect the tumor microenvironment and cancer stem cells (Qin *et al.*, 2024). Therefore, understanding the regulatory mechanism of AEG in CRC is vital for the prevention and treatment of CRC.

Phosphatidylinositol-3-kinase (PI3K) / protein kinase B (Akt) is the most frequently activated signaling pathway in human cancers (Glaviano *et al.*, 2023). PI3K/Akt pathway can be activated by a variety of factors that affect the AEG pathway and thus plays an important role in the proliferation, metastasis and drug resistance of CRC (Su,

**Corresponding author:* e-mail: MingliaoNiu123456@hotmail.com

2022; Sun *et al.*, 2022; Wang *et al.*, 2024; Wang *et al.*, 2023). The decrease of replication factor C subunit 2 (RFC2) expression can inhibit the expressions of lactate dehydrogenase A (LDHA), glucose transporter-1 (GLUT1) and hexokinase2 (HK2), which are key to the AEG pathway in CRC cells, indicating that RFC2 enhances the AEG pathway of CRC by promoting the PI3K/Akt pathway (Lou and Zhang, 2023). In the AEG, protein53 (P53) is a crucial upstream regulator and is important for the prognosis of CRC. IC261 can reduce the expression of P53 protein in CRC cells. After using the P53 inhibitor, IC261-induced AEG can be reduced, which once again proved that P53 is involved in the regulation of AEG as a regulatory factor (Hou *et al.*, 2023; Liu *et al.*, 2015; Liu *et al.*, 2020). In conclusion, PI3K/Akt/P53 pathway is important for AEG of CRC.

Cantharidin and norcantharidin have good anti-tumor activity and can play a role in enhancing proliferation, promoting apoptosis and anti-glycolysis in liver cancer and colorectal cancer (Feng *et al.*, 2018; Yan *et al.*, 2023; Zhang *et al.*, 2020). However, there are few reports on the antitumor activity of cantharidic acid (CA). CA inhibits the growth of oral squamous cell carcinoma and induces apoptosis of leukemia HL-60 cells through endoplasmic reticulum stress and caspase-3 activation (Wang *et al.*, 2018; Xi *et al.*, 2015). In addition, CA can also induce apoptosis of SK-Hep-1 cells through P38-mediated apoptosis (Feng *et al*., 2018). Therefore, CA has anti-tumor activity.

In the network pharmacology analysis, we found that the anti-CRC effect of CA was closely related to the PI3K/Akt pathway. In this study, CRC cells were used as the research objects and CA was used for treatment. The malignant progression of cells, the expressions of AEG and the PI3K/Akt/P53 pathway were analyzed and the effect of CA on the development of CRC was verified by constructing a mouse xenograft model. The purpose of this study is to elucidate the mechanism by which CA influences the development of CRC by regulating glycolysis and to provide references for the diagnosis and treatment of CRC.

MATERIALS AND METHODS

Cell culture and treatment

Human normal colorectal mucosal cells FHC were purchased from Chemical Book (C0334, Shanghai, China) and human CRC cell lines (SW480 and HT29) were purchased from Procell (CL-0223, CL-0118, Wuhan, China). The cells were cultured in DMEM medium containing 10% fetal bovine serum (FBS, R999297, MACKLIN, Shanghai, China). Cells in the logarithmic growth phase were used for experiments.

FHC cells (1×10^4 cells/well) were seeded into 96-well plates. After the cells were fully adherent, 0, 1.25, 2.5, 5, 10, 20 and 40 μM CA were added to incubate for 24 h, then 10 μL cell counting kit-8 (CCK-8) solution (CA1210, Solarbio, Beijing, China) was added. The cells were incubated for 2 h, the wavelength of 450 nm was selected. The light absorption (OD) value was measured on a microplate reader (51119770 DP, HITACHI, Japan) and the cell survival rates were calculated. The safe concentration range of CA was screened.

SW480 and HT29 cells were divided into Control group, 5, 10, 20 μM CA intervention group, 20 μM CA+6-phosphofructo-2-kinase/fructose-2,6-biphosphatase 3 (PFKFB3) overexpression (CA+PFKFB3) group and negative control (CA+Vector) group, 20 μM CA+PI3K activator 740 Y-P (CA+740 Y-P) group. Flag-PFKFB3 was constructed into pCDH lentiviral expression vector to infect SW480 and HT29 cells. After 48 hours of infection, 1 μg/mL puromycin (S7417, Selleck, Shanghai, China) was added to screen the infected cells. The cell lines expressing empty vector (Vector group) and Flag-PFKFB3 (PFKFB3 overexpression group) were obtained. The expression level of PFKFB3 protein was verified by Western blot. The cells (1×10^4 cells/well) were seeded into 96-well plates and incubated with 5, 10, 20 μM CA and 10 μM 740 Y-P (HY-137135, HY-P0175, MedChemexpress MCE, New Jersey, USA) for 24 h. The $OD_{450\ nm}$ value was detected by CCK-8 and calculate the cell survival rates.

5-Ethynyl-2'-deoxyuridine (EdU) detection

The treated SW480 and HT29 cells were collected and cultured with 10 μM EdU for 12 h. Cells were fixed with methanol. According to the instructions of the EDU cell proliferation assay kit (C10310-1, RiboBio, Guangzhou, China), the cells were permeabilized, washed, 4',6-diamidino-2'-phenylindole (DAPI)-stained and observed under a fluorescence microscope (BX63, OLYMPUS, Shanghai, China). The cell proliferation rate was represented by the positive ratio of EdU staining, using unintervened SW480 and HT29 cells as controls. The experiment was repeated three times independently.

Clone formation experiment

The CRC cells were seeded into 6-well plates at 200 cells/well. Three wells were set in each group. DMEM+10% FBS medium was used. The next day, the medium was changed and observed. When the diameter of the clone in the culture dish was about 1-2 mm, the culture was terminated and fixed with 4% paraformaldehyde (PFA) for 15 min. Finally, 0.1% crystal violet (G1014, Servicebio) was added and stained for 15 min. The cells were photographed under an air-dried microscope and the number of clones was counted, using unintervened SW480 and HT29 cells as controls.

Transwell test

Migration assay: the cells were cultured in serum-free medium for 24 h, digested with 0.25% trypsin and made into cell suspension. The cell suspension was added to the upper chamber of Transwell and 500 μL of complete

medium containing 10% FBS was added to the lower chamber of Transwell. After 24 h of culture in a cell incubator, the upper chamber matrigel and cells were wiped off and the cells migrated to the lower chamber were fixed for 15 min and stained for 15 min with 4% PFA and 0.1% crystal violet (G1014, Servicebio) staining solution, respectively. The chamber was observed under a microscope and the number of cells passing through the chamber membrane was counted by Image J software, using unintervened SW480 and HT29 cells as controls.

Invasion assay: Matrigel was diluted in serum-free medium, coated on polycarbonate membrane in the upper chamber of Transwell chamber at 50 μL/well and polymerized at 37°C for 4 h. Other steps were the same as migration assay.

Flow cytometry

The treated CRC cells (SW480 and HT29) were incubated with 5 μL Annexin V-APC and PI (88-8007-74, eBioscience) in darkness for 10 min and the apoptotic cells were tested using flow cytometry (Attune, ThermoFisher, Shanghai, China), using unintervened SW480 and HT29 cells as controls. The experiment was repeated three times independently.

LDH detection

CRC cells were cultured in 96-well plates to grow to 80%. The LDH kit (C0016, Beyotime, Shanghai, China) was used to prepare the corresponding solution and 60 μL LDH release reagent was added. After incubation in a cell incubator for 1 h, 120 μL supernatant was taken and added to the corresponding hole of the new 96-well plate. The OD value was measured at 490 nm of the microplate reader and the LDH release amount in the cell culture medium of each group was calculated according to the formula, using unintervened SW480 and HT29 cells as controls. The experiment was repeated three times independently.

Hoechst 33258 fluorescence staining

The medium of treated cells was removed and fixed with 4% PFA for 10 min. After rinsing with pre-cooled PBS, 100 μL Hoechst 33258 dye (KGA1802, KeyGEN BioTECH, Jiangsu, China) was added to each hole for 10 min oscillation. After 2-3 times of pre-cooling PBS washing, a drop of fluorescent sealant was added to the glass slide. Observe and take pictures under inverted fluorescence microscope. Unintervened SW480 and HT29 cells were used as control.

Cell cycle detection

SW480 and HT29 cells were collected and resuspended in 0.5 mL PBS, slowly fixed with 4.5 mL of pre-cooled 70% ethanol and placed in a refrigerator at -20°C overnight. On the next day, 0.5 mL PI staining solution containing RNase A was added and incubated at 37°C in dark for 30 min. The cell cycle was detected by flow cytometry and the experiment was repeated for 3 times.

AEG index detection

The cells were collected and ultrasonically disrupted with the extract. After centrifugation, the supernatants were taken for detection. The glucose uptake assay kit and lactic acid assay kit (ab136955, ab65331, abcam) were used to detect the OD value of each well under the microplate reader according to the manufacturer's instructions and the glucose uptake and lactic acid production in cells were calculated, using unintervened SW480 and HT29 cells as controls. The experiment was repeated three times independently.

The extracellular acidification rate (ECAR) was measured using the Seahorse XF 96 Extracellular Flux Analyzer (Agilent, USA) according to the instructions of the kit (ab197244, abcam). 1×10^4 cells per well were seeded in a Seahorse XF cell culture plate, after baseline measurement. Glucose, oxidative phosphorylation inhibitor oligomycin and glycolysis inhibitor 2-DG were added at each specified time point to detect ECAR. The data were evaluated by Seahorse XF-96 Wave software and expressed as mpH/min, using unintervened SW480 and HT29 cells as controls. Each curve of each hole was repeatedly measured three times.

Western blot (WB)

The cells and transplanted tumors were collected and the total protein was extracted with RIPA lysis buffer. The protein concentration was determined using BCA kit. A total of 20 μg protein was loaded, transferred to PVDF membrane after electrophoresis, blocked with 5% skim milk for 1 h and incubated with primary antibodies Bax (ab182733, abcam), Bcl2 (ab692, abcam), caspase-3 (ab32351, abcam), Cleaved caspase-3 (ab208003, abcam), caspase-9 (ab185719, abcam), Cleaved caspase-9 (9507, Cell Signaling, Danvers, MA, USA), GLUT1 (ab115730, abcam), HK2 (ab104836, abcam), LDHA (19987-1-AP, proteintech, Wuhan, China), PFKFB3 (ab181861, abcam), PI3K (4292, Cell Signaling), p-PI3K (4257, Cell Signaling), Akt(ab314110, abcam), p-Akt(ab314038, abcam), P53 (ab32048, abcam), PCNA (ab92552, abcam), Ki67 (ab16667, abcam), MMP3 (ab52915, abcam), MMP9 (ab58803, abcam) and GAPDH (ab9485, abcam) at 4°C overnight. The secondary antibody was added and incubated for 2 h. ECL imaging was performed. The protein gray value was analyzed by Image J software and GAPDH was used as internal reference. The relative expression of protein was calculated.

Molecular docking

The structures of AKT1 (7WM2) and TP53 (1XNI) were obtained by RCSB PDB database (https://www.rcsb.org/) and the 3D structure information of CA was obtained by PubChem database (http://pubchem.ncbi.nlm.nih.gov/). After the target protein and small molecule were processed by AutuDock Tools 1.5.6 software, the target protein and small molecule were docked by Autudock Vina and the

target protein and small molecule with good docking results were visualized by PyMol 2.3.4 software.

Nude mouse model of transplanted tumor

Twenty 5-week-old SPF BALB/c nude mice, male, provided by Slack Laboratory Animals Co., Ltd. (Shanghai, China), were bred in Henan Provincial Hospital of Traditional Chinese Medicine Animal Experimental Center. This study was approved by Nanyang Medical College Ethics Committee (No. 2025-0011, date: 2025.1.17).

SW480 cells in good logarithmic growth phase were collected and single cell suspension with a density of 5×10^6/mL was prepared using PBS solution. Twenty nude mice were subcutaneously injected according to the principle of sterility. The total volume of each nude mouse was 0.2 mL and the inoculation site was the right posterior axillary. After the subcutaneous formation of the naked eye, the needle was pulled out and the cotton ball was temporarily pressed on the injection site to avoid the outflow of cell suspension. Nude mice were randomly divided into control group and CA low, medium and high dose groups, with 5 mice in each group. CA groups were intraperitoneally injected with 0.2, 0.3 and 0.4 mg/kg CA every day, while the control group was intraperitoneally injected with the corresponding normal saline. The tumor diameter was measured with a vernier caliper every 7 days after inoculation and the tumor volume ($1/2\times length\times width^2$, mm^3) was calculated. After 28 days, the transplanted tumor tissue was removed after anesthesia in nude mice and the tumor weight was weighed.

Terminal deoxynucleotidyl transferase dUTP nick-end labeling (TUNEL)

The tumor was fixed in 4% PFA, dehydrated, embedded in paraffin and sliced. The slices were dewaxed with xylene and rehydrated with gradient ethanol for 3 min each time. Rinse with PBS, add protease K working solution for 50 min. TUNEL staining was performed following TUNEL kit instructions. After the slide was dried, 50 μL converter-POD was added to the specimen and the cover glass was added and reacted for 50 min in a dark box. DAB substrate was added and the reaction was carried out at room temperature for 10 min. After hematoxylin counterstaining, the samples were washed with tap water immediately. After gradient alcohol dehydration, xylene transparent, neutral gum sealing. TUNEL positive cells were observed under a microscope. Untreated transplanted tumor nude mice were used as control.

Immunohistochemistry

Paraffin sections were baked and deparaffinized in turn to water and then incubated with 100 μL 3% H_2O_2 solution for 10 min. They were placed in boiling antigen repair solution for 15 min and 5% BSA was added to block the circle for 20 min. Primary antibodies Ki-67 (ab92742, abcam), Cleaved caspase-3 (25128-1-AP, proteintech) and Cleaved caspase-9 (9507, Cell Signaling) were incubated overnight at 4℃. The cells were incubated with secondary antibody for 50 min. DAB coloration and hematoxylin counterstaining were performed. The protein expressions were calculated by Image J image analysis system. Untreated transplanted tumor nude mice were used as control. The experiment was repeated three times independently.

Immunofluorescence

After the paraffin sections were blocked for 30 min, the primary antibody GLUT1 (ab115730, abcam) was incubated overnight at 4ºC and the fluorescent secondary antibody (ab150077, abcam) was incubated for 1 h in the dark. The tablet (S2110, Solarbio) was sealed and the fluorescence signal was observed by fluorescence microscope and the image was analyzed by Image J. Untreated transplanted tumor nude mice were used as control. The experiment was repeated three times independently.

STATISTICAL ANALYSIS

SPSS 26.0 software was used for statistical analysis of the data and the measurement data with normal distribution were expressed as mean ±standard deviation. One-way ANOVA analysis was used to compare the quantitative data between groups and $P < 0.05$ was considered statistically significant.

RESULTS

CA inhibited the growth, movement and invasion of CRC cells

SW480 and HT29 cells are commonly used cells for CRC cell experiments. In this study, FHC cells were used as controls to explore CA impact on CRC. The structural formula of CA was displayed in fig.1A. We first explored the safety of CA. When FHC cells were treated with different concentrations of CA for 24 h, CCK-8 detected no significant difference in FHC cell viability, indicating that the dose of CA used in this study did not damage normal cells; however, the cell viability decreased slightly when the dose of CA was 40 μM (fig.1B), so 5, 10 and 20 μM CA were selected for the following tests. After that, we used CA to intervene SW480 and HT29 cells and CCK-8 detected a notable decline in the viability of CRC cells (SW480 cells (81.00±5.56)%, (67.33±5.51)% and (54.00±8.54)%), HT29 cells (78.00±7.00)%, (66.33±6.51) % and (48.33±8.50)%), fig.1C-D); the proportion of EdU positive cells (SW480 cells (61.23±6.63)%, (45.77±6.52) % and (25.15±10.22)%), HT29 cells (29.77±8.51)%, (38.67±7.50)% and (27.00±7.21)%), fig.1E-G) and the number of colony formation (SW480 cells (214.67±21.03), (163.00±23.00) and (103.33±38.84), HT29 cells (225.00±25.00), (178.33±25.17) and (126.00±23.52), fig.1H-J) were also significantly reduced, indicating that CA could reduce the proliferation rate of CRC cells.

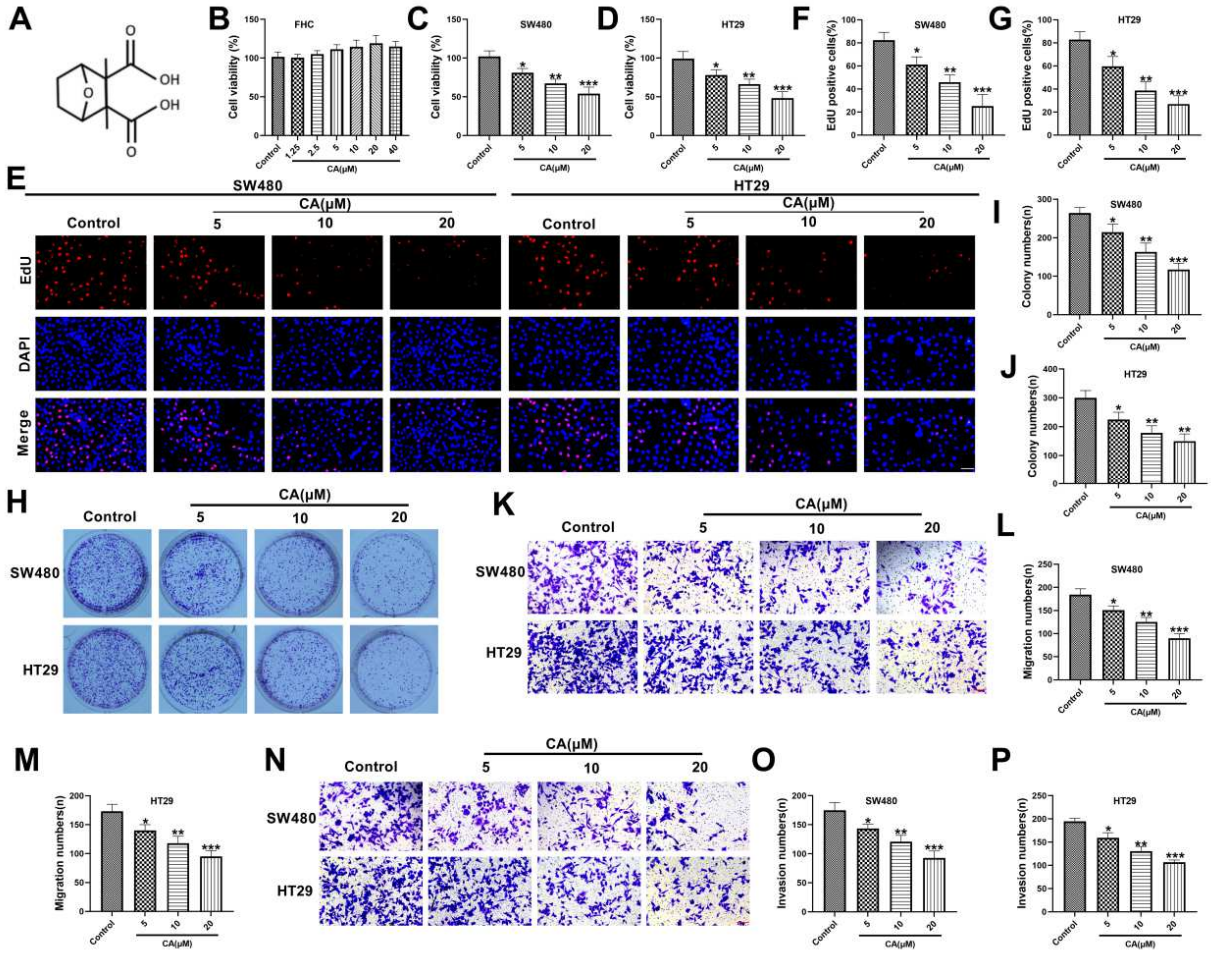

Fig. 1: CA inhibited the growth, movement and invasion of CRC cells
A: CA structural formula.
B: The viability of FHC cells was discovered through the CCK-8 test after 0-40 μM CA intervention for 24 h.
C-D: The viability of SW480 and HT29 cells was detected using CCK-8 assay after CA intervention.
E-G: The proliferation of CRC cells when CA intervention was detected by EdU assay (×40, 50 μm).
H-J: The growth of SW480 and HT29 cells when CA treatment were detected by cell colony formation assay.
K-P: The movement and invasion of CRC cells after PA treatment were detected by Transwell experiment (×20, 100 μm).
n=3, **P* < 0.05, ***P* < 0.01, ****P* < 0.001 vs Control group.

CA obviously reduced the number of the movement (SW480 cells (151.00±9.00), (125.00±10.00) and (90.33±9.50), HT29 cells (140.33±10.01), (118.00±12.00) and (95.33±9.50), fig.1K-M) and invasion cells (SW480 cells (143.33±7.64), (120.67±11.02) and (92.67±12.01), HT29 cells (159.33±11.02), (130.67±10.02) and (106.67±4.93), fig.1N-P). In addition, this study also found that the expression levels of proliferation-related proteins PCNA, Ki67 and invasion-related proteins MMP3 and MMP9 were decreased after CA intervention (fig.S1A-C). The above experiments showed that CA weakened the growth, movement and invasion of CRC cells, suggesting that CA had a tumor suppressor effect.

CA induced apoptosis of CRC cells

In this study, SW480 and HT29 cells were given 5, 10 and 20 μM CA for 24 h. The cell apoptosis rate (SW480 cells (20.95±1.87)%, (33.04±2.08)% and (45.91±3.15)%), HT29 cells (13.70±2.73)%, (23.13±1.73)% and (31.73±3.01)%), fig.2A-C) and LDH release (SW480 cells (28.33±3.51)%, (36.00±4.00)% and (46.00±3.61)%), HT29 cells (32.00±4.00)%, (42.00±5.00)% and (52.00±3.46)%), fig.2D-E) were significantly increased, suggesting that CA could induce apoptosis of CRC cells. Hoechst 33258 penetrates cell membrane. It releases strong blue fluorescence after embedding double-stranded DNA, which is commonly used in apoptosis detection. The results of this study showed that untreated CRC cells grew well, had a strong wall apposition and showed a uniform blue fluorescence; after the intervention of CA, some of the cells showed a bright blue fluorescence and apoptotic vesicles appeared, therefore, CA could significantly increase the intensity of Hoechst 33258 fluorescence (fig.2F-H).

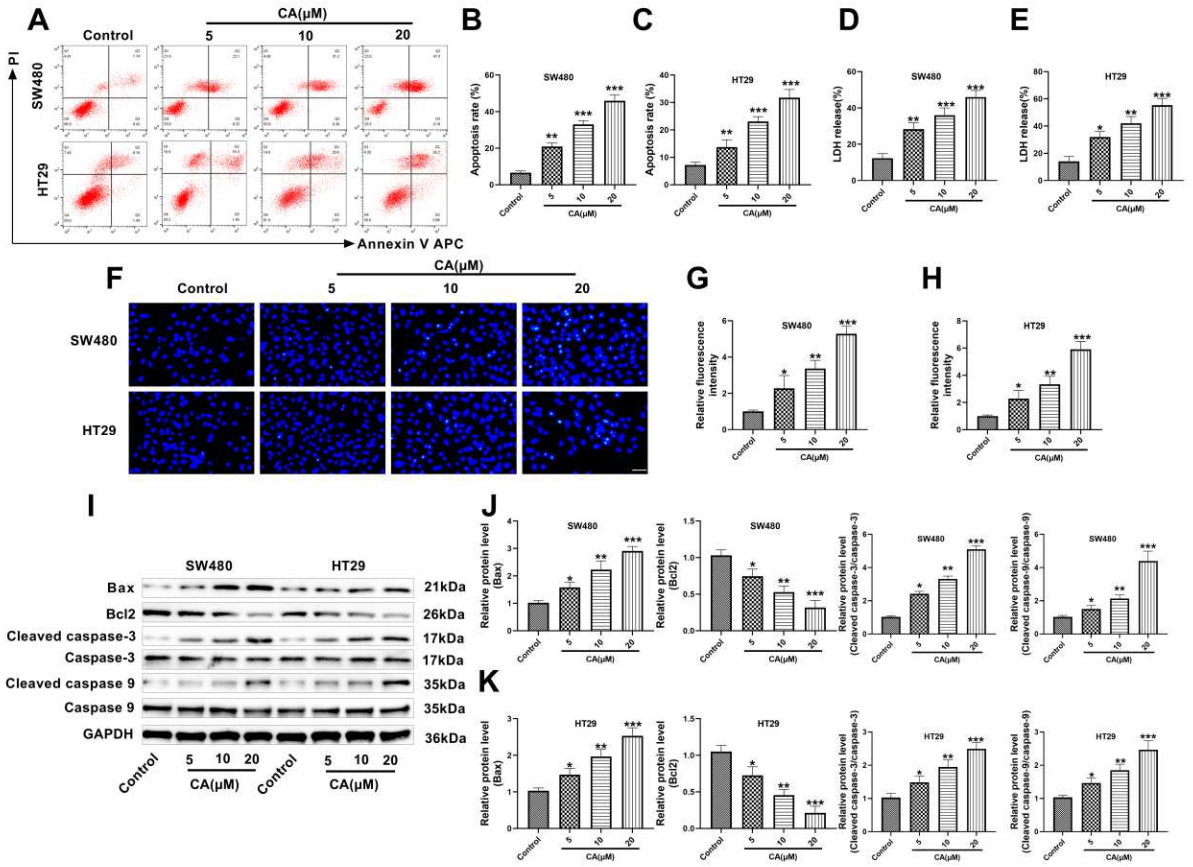

Fig. 2: CA induced apoptosis of CRC cells
A-C: The apoptosis of SW480 and HT29 cells was detected by flow cytometry.
D-E: LDH release assay was used to detect the apoptosis.
F-H: The apoptosis of CRC cells was detected by Hoechst 33258 fluorescence staining after CA intervention for 24 h (×40, 50 μm).
I-K: WB was used to detect the expression of Bax, Bcl2, caspase-3, caspase-9, Cleaved caspase-3 and Cleaved caspase-9.
n=3, *$P < 0.05$, **$P < 0.01$, ***$P < 0.001$ vs Control group.

After that, the levels of Bax, Cleaved caspase-3 and Cleaved caspase-9 were raised when CA therapy and the level of Bcl2 protein was decreased (fig.2I-K). The above experiments showed that CA could promote the apoptosis of CRC cells. And CA also effectively triggered cell cycle arrest, CA effectively decreased the number of cells in G1 phase and increased the number of cells in G2 phase (fig.S2A-C). In conclusion, CA inhibited the malignant progression of CRC cells.

CA inhibited the AEG of CRC cells and inhibited the malignant progression of CRC

Since 20 μM CA had the most obvious anti-tumor effect, this concentration was selected for subsequent mechanism research. More and more studies have shown that AEG is related to tumor migration, invasion and drug resistance and AEG metabolism is considered to be a new direction for anticancer therapy. In this study, it was found that the glucose uptake and AEG final product lactic acid production of SW480 and HT29 cells were significantly decreased after CA treatment (fig.3A-B). Then, ECAR was detected in this study, which could detect the changes of glucose metabolism in real time. CA could reduce the ECAR value of cells (fig.3C), suggesting that the glycolysis ability was weakened, indicating that CA could inhibit the AEG ability of CRC cells. Next, the glycolysis-related proteins were detected. CA significantly lessened the protein levels of GLUT1, HK2, LDHA and PFKFB3 (fig.3D-E). CA effectively inhibited AEG in CRC cells.

PFKFB3 is a key activator of glycolysis, PFKFB3 in CRC cells was overexpressed in this study. WB showed that PFKFB3 was effectively overexpressed, suggesting that the stable cell line overexpressing PFKFB3 was successfully constructed (fig.4A-B). CRC cells overexpressing PFKFB3 were given 20 μM CA. Compared with CA alone, PFKFB3 overexpression significantly increased the number of colony formation (SW480 cells (117.67±16.17), (113.67±16.80) and (200.33±10.50), HT29 cells (150.67±26.00), (156.00±31.43) and (236.67±15.28), fig.4C-D), migration (SW480 cells (90.33±10.02), (91.33±8.62) and (130.00±11.14), HT29 cells (95.00±9.00), (92.00±9.54) and (134.00±8.54), fig.4E-F) and invasion cells.

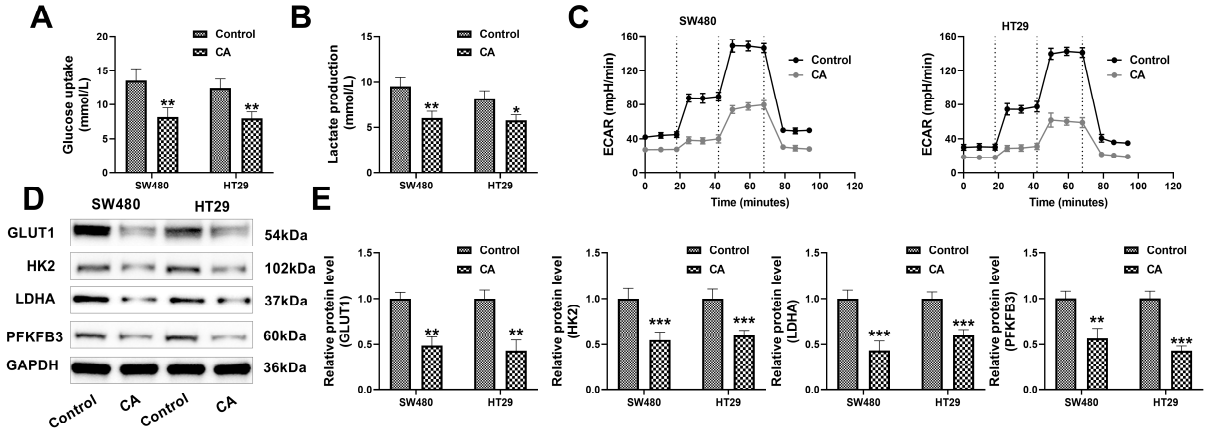

Fig. 3: CA inhibited AEG of CRC cells
A-B: The glucose uptake and lactic acid production of SW480 and HT29 cells were detected by the kit.
C: The ECAR levels were evaluated by ECAR kit.
D-E: The expressions of glycolysis-related proteins GLUT1, HK2, LDHA and PFKFB3 were detected by WB.
n=3, *$P < 0.05$, **$P < 0.01$, ***$P < 0.001$ vs Control group.

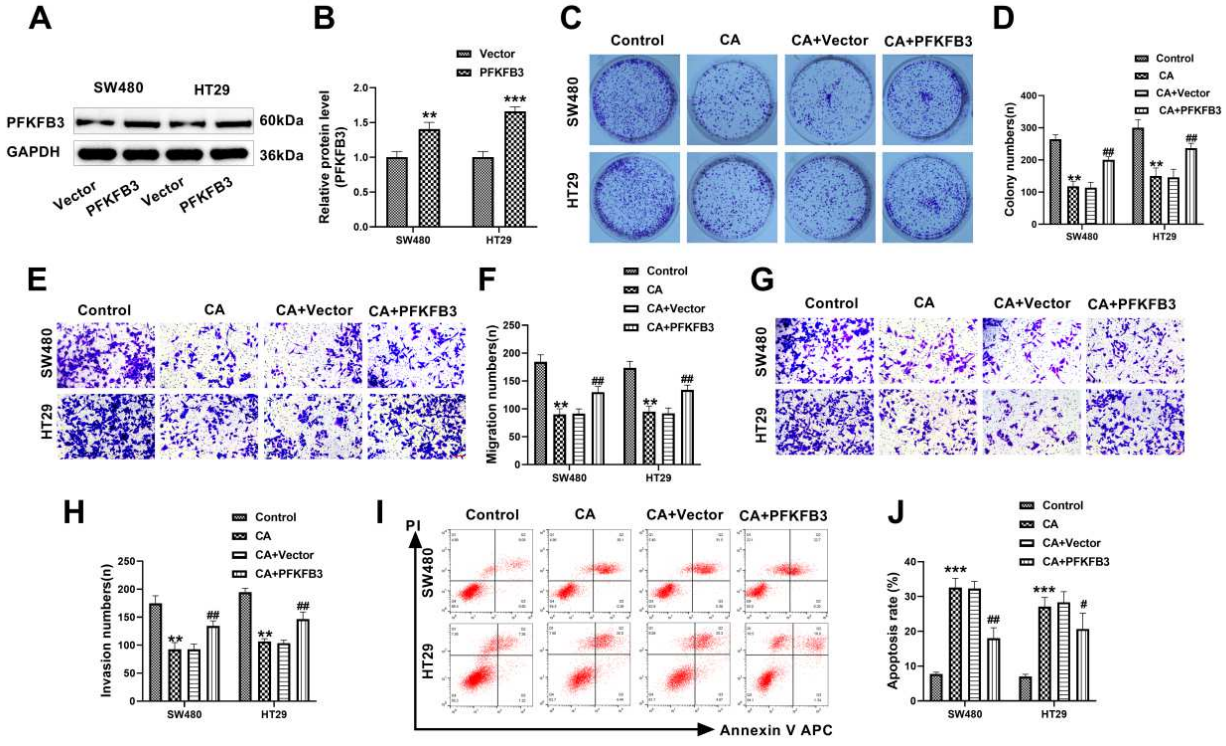

Fig. 4: CA inhibited the AEG of CRC cells and inhibited the malignant progression of CRC
A-B: The overexpression vector of PFKFB3 was constructed and transfected into SW480 and HT29 cells. The transfection efficiency was detected by WB.
C-D: The proliferation of cells after transfection was detected by cell clone formation assay.
E-H: The movement and invasion of cells after transfection were detected by Transwell experiment (×20, 100 μm).
I-J: The apoptosis of cells when transfection was tested by flow cytometry.
n=3, **$P < 0.01$, ***$P < 0.001$ vs Control group; #$P < 0.05$, ##$P < 0.01$ vs CA+Vector group.

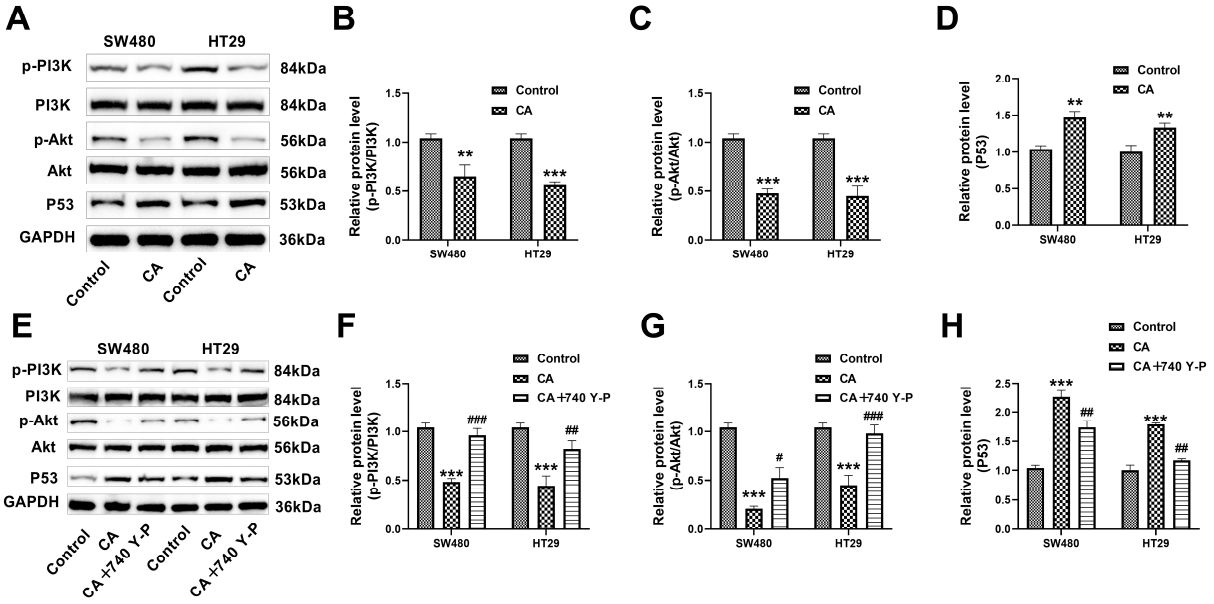

Fig. 5: CA controlled the PI3K/Akt/P53 pathway
A-B: The levels of PI3K, p-PI3K, Akt, p-Akt and P53 in the PI3K/Akt/P53 pathway were detected by WB.
C-D: The expressions of PI3K/Akt/P53 pathway proteins after 740 Y-P treatment were detected by WB.
n=3, **$P < 0.01$, ***$P < 0.001$ vs Control group; #$P < 0.05$, ##$P < 0.01$, ###$P < 0.001$ vs CA group.

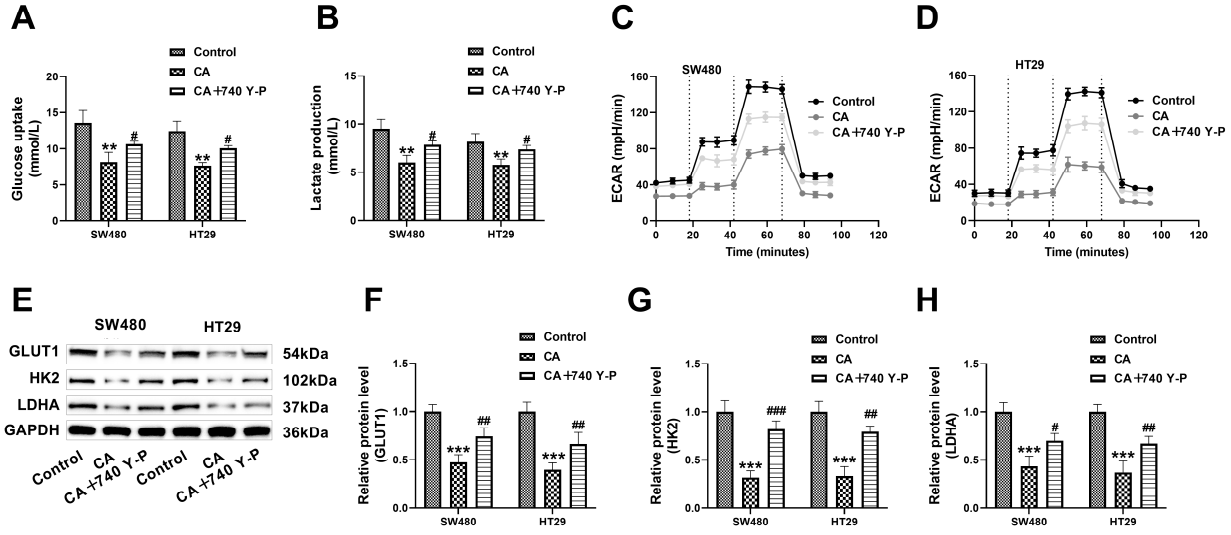

Fig. 6: CA inhibited AEG in CRC cells through the PI3K/Akt/P53 pathway
A-B: SW480 and HT29 cells were treated with PI3K activator 740 Y-P for 24 h. The glucose uptake and lactic acid production were detected by the kit.
C: The ECAR levels of cells were evaluated by ECAR kit.
D-E: The expressions of GLUT1, HK2 and LDHA were detected by WB.
n=3, **$P < 0.01$, ***$P < 0.001$ vs Control group; #$P < 0.05$, ##$P < 0.01$ vs CA group.

(SW480 cells (92.67±12.01), (92.67±9.29) and (134.33±9.02), HT29 cells (106.67±4.93), (103.67±5.13) and (146.67±12.58), fig.4G-H) and significantly decreased the apoptosis rate (SW480 cells (32.57±2.67)%, (32.33±2.07)% and (18.00±3.10)%), HT29 cells (27.07±2.66)%, (28.33±3.06)% and (20.97±4.50)%), fig.4I-J), indicating that PFKFB3 overexpression promoted the growth, movement and invasion of CRC cells and inhibited apoptosis, indicating that PFKFB3 overexpression could weaken the anti-cancer effect of CA. In conclusion, CA inhibited the malignant progression of CRC by inhibiting the AEG.

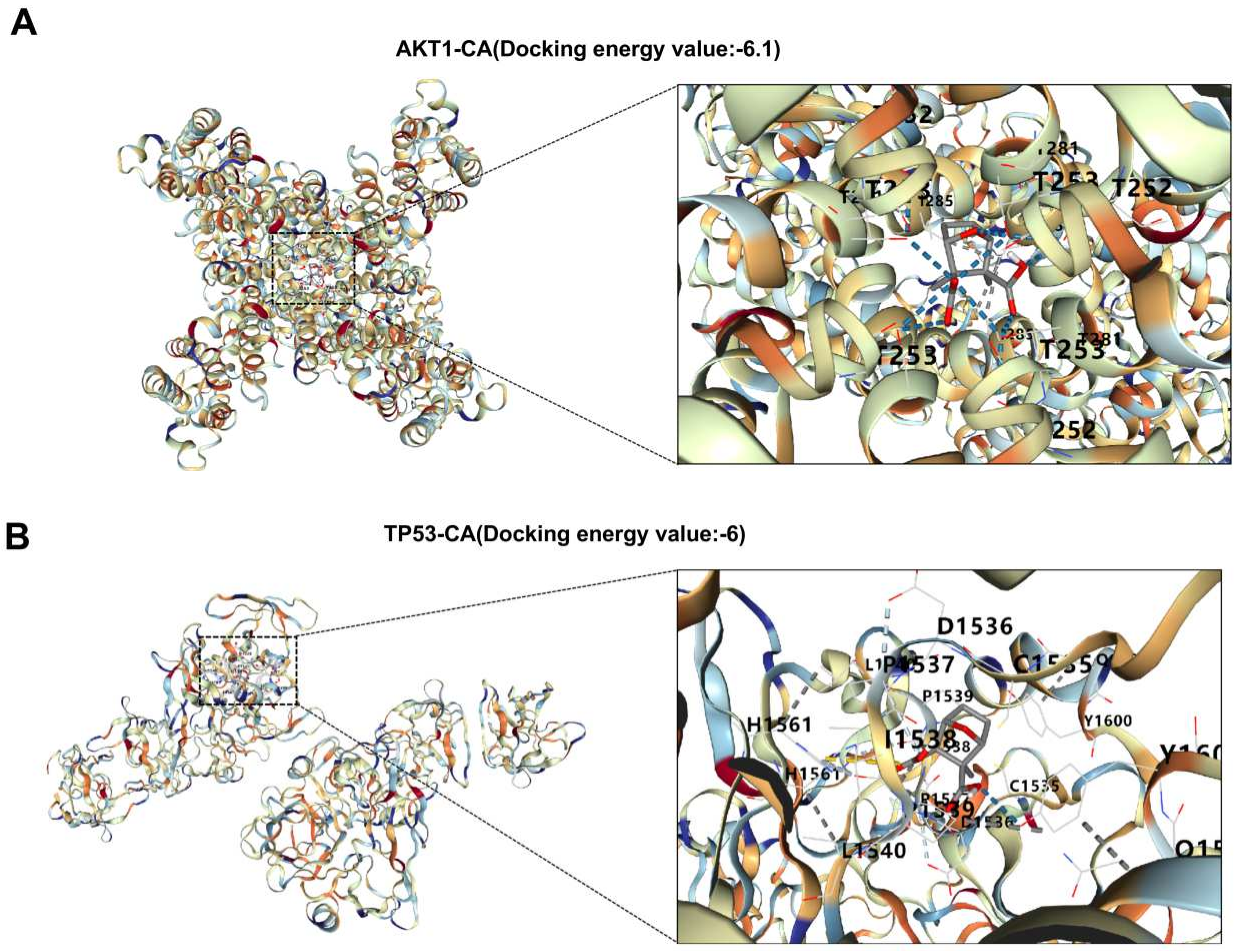

Fig. 7: Molecular docking prediction of CA with AKT1 and TP53
A-B: The molecular docking diagram of CA and target proteins (AKT1 and TP53), the left side was the overall binding diagram, and the right side was the detailed binding diagram.

CA inhibited AEG in CRC cells through the PI3K/Akt/P53 pathway

After CA intervention, the levels of p-PI3K and p-Akt were declined and the level of P53 protein was increased (fig.5A-D), CA regulated the PI3K/Akt/P53 pathway. In order to explore whether CA inhibited AEG was related to the PI3K/Akt/P53 pathway, CRC cells were given 10 μM PI3K activator 740 Y-P while CA intervened. Compared with CA alone intervention, 740 Y-P significantly raised p-PI3K and p-Akt levels and decreased P53 protein level (fig.5E-H). In addition, this study also found that 740 Y-P increased glucose uptake, lactate production (fig.6A-B) and the ECAR value (fig.6C-D), suggesting that 740 Y-P could promote AEG of CRC cells. In addition, the levels of GLUT1, HK2 and LDHA were also increased after 740 Y-P treatment (fig.6E-H). In summary, CA could inhibit AEG in CRC cells by regulating the PI3K/Akt/P53 axis.

Molecular docking prediction of CA with AKT1 and TP53

The lower the binding energy of ligand and receptor docking is, the more stable the molecular binding is. When the binding energy is ≤ -5.0 kcal/mol, the binding is more stable and the lower the value is, the better the binding is. After docking of CA with AKT1 and TP53, the molecular docking results showed that the binding energies of CA with AKT1 and TP53 were -6.1 and -6.0 kcal/mol and the docking binding energy of CA with AKT1 and TP53 was < -5.0 kcal/mol, indicating that the ligand and receptor had stable binding activity. CA might play an anti-cancer role through AKT1 and TP53. fig.7 showed its visual docking mode.

CA inhibited the malignant progression of CRC through the PI3K/Akt/P53 signaling pathway in vivo

Given that CA inhibited CRC *in vitro*, this study would further verify the anti-tumor effect of CA in nude mice. The subcutaneous tumor-bearing model of nude mice was established by subcutaneous injection of SW480 and 0.2, 0.3 and 0.4 mg/kg CA was injected intraperitoneally every day for treatment. After 28 days, the mice were sacrificed.

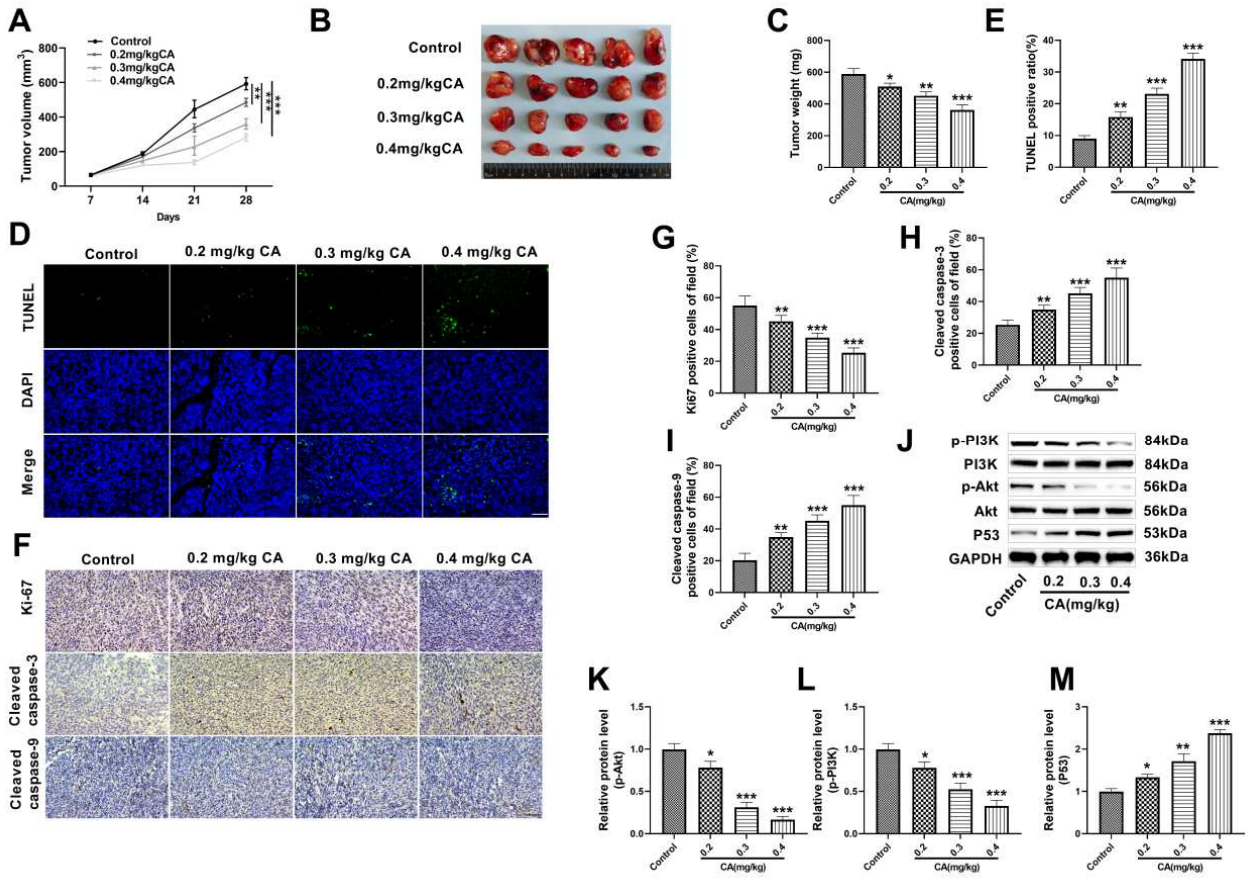

Fig. 8: CA inhibited the malignant progression of CRC through the PI3K/Akt/P53 pathway *in vivo*

A-C: Subcutaneous injection of SW480 cells was used to construct a nude mouse xenograft model, and CA was injected intraperitoneally, and then the size and weight of the tumor were measured.

D-E: The number of TUNEL positive cells in tumor tissues was detected using TUNEL (×40, 50 μm).

F-I: The expressions of Ki-67, Cleaved caspase-3 and Cleaved caspase-9 in tumor tissues were detected by immunohistochemistry (×40, 50 μm).

J-M: The expression of PI3K/Akt/P53 pathway proteins in the tumor was detected by WB.

n=5, *$P < 0.05$, **$P < 0.01$, ***$P < 0.001$ vs Control group.

After CA treatment, the weight and volume of transplanted tumors in mice were reduced (fig.8A-C), TUNEL, Cleaved caspase-3 (34.92±2.83)%, (45.18±3.72)% and (55.00±6.08)%) and Cleaved caspase-9 (35.02±2.75)%, (44.98±4.01)% and (55.11±5.88)%) positive cells in transplanted tumors were increased and Ki-67 positive cells (45.18±3.72)%, (34.92±2.83)% and (25.34±3.11)%) were significantly decreased (fig.8D-I), indicating that CA inhibited the growth of CRC cells *in vivo* and promoted the apoptosis of transplanted tumors. In addition, this study also found that CA significantly reduced the expressions of p-PI3K and p-Akt in transplanted tumors and raised the expression of P53 protein (fig.8J-M), indicating that CA regulated the PI3K/Akt/P53 axis *in vivo*. The above experiments showed that CA could regulate the PI3K/Akt/P53 axis *in vivo*, thereby inhibiting the malignant progression of CRC.

CA inhibited AEG through PI3K/Akt/P53 signaling pathway

Moreover, we also found that after CA intervention, the fluorescence intensity of GLUT1 (fig.9A-B) and the expressions of GLUT1, HK2 and LDHA proteins (fig.9C-F) in transplanted tumors of mice were significantly reduced, indicating that CA could also inhibit AEG *in vivo*. Combined with the results of previous cell experiments, it is showed that CA inhibited AEG via the PI3K/Akt/P53 pathway and then treated CRC.

DISCUSSION

The occurrence and development of colorectal cancer is a multi-gene complex process. Its early condition is hidden. Most patients have reached the late stage when they are treated and even metastasis occurs, resulting in a greatly reduced survival rate of patients and the prognosis is not ideal.

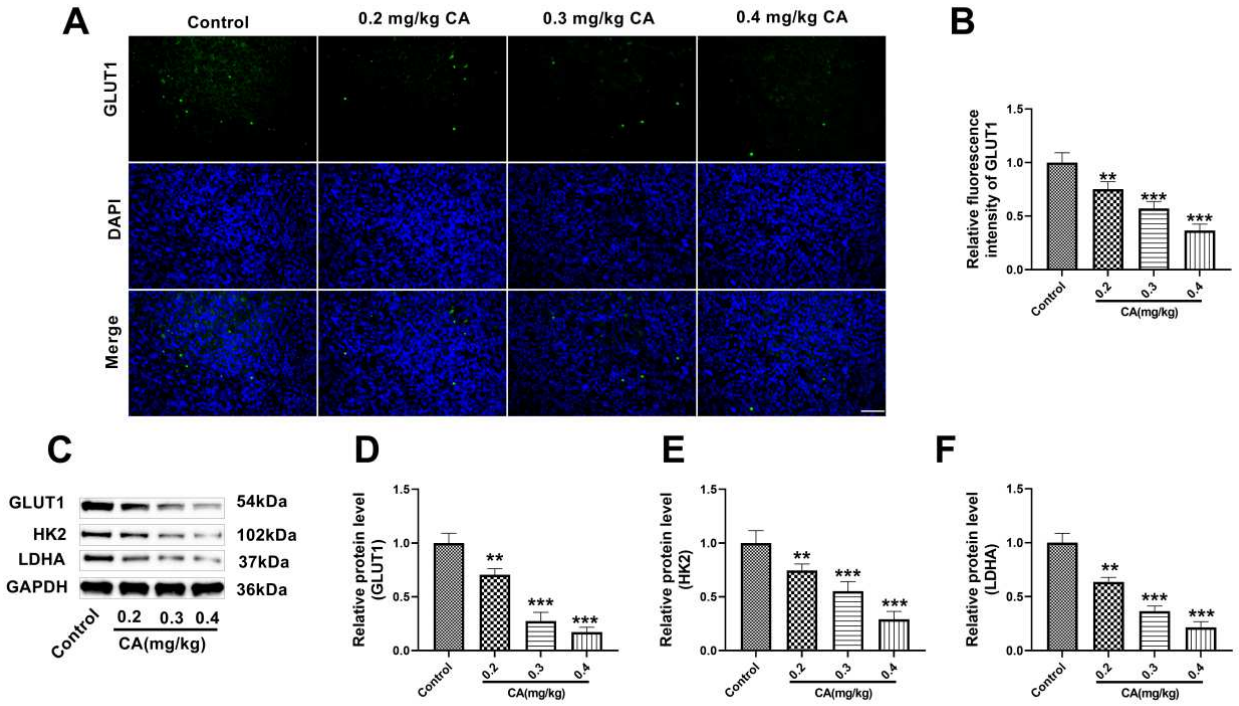

Fig. 9: CA inhibited AEG through PI3K/Akt/P53 pathway
A-B: The expression of GLUT1 in the transplanted tumor was detected by immunofluorescence (×40, 50 μm).
C-F: The expressions of GLUT1, HK2, LDHA and PFKFB3 in tumors were detected by WB.
n=5, $^{**}P < 0.01$, $^{***}P < 0.001$ vs Control group.

It is particularly vital to explore a therapy method. Cell proliferation is an important intrinsic property of the body to maintain the homeostasis of the internal environment. It maintains the relative constant of cell types and cell numbers in various organs. Therefore, once it is disordered, it will lead to the occurrence of many diseases and the excessive proliferation of cells has always been considered to be the main reason for the sustainable development of cancer. Therefore, it is the main direction and hot spot of cell biology research to study and reveal the related regulation mechanism of cell proliferation. The hallmark feature of cancer is abnormal cell proliferation and metastasis. This study found that CA inhibited the proliferation, migration and invasion of CRC cells, indicating that CA had an anti-CRC effect.

Apoptosis is the programmed cell death controlled by genes, which ensures the normal growth and development of organisms and maintains tissue homeostasis. When apoptosis is dysregulated, tumor cells escape the surveillance of the immune system and promote their malignant proliferation and metastasis (Pu *et al.*, 2021). Bcl2 family proteins are an important class of proteins in the regulation of apoptosis. The family mainly includes the apoptosis inhibitory protein Bcl2 and the apoptosis promoting protein Bax. Studies have found that under the stimulation of exogenous or endogenous apoptotic signals, Bcl2 can form a Bcl2-Bax dimer by binding to Bax. The expression of Bcl2 is up-regulated, forming a heterodimer with Bax, the release of cytochrome C (Cyt C) is inhibited and apoptosis is blocked. When the expression of Bax is up-regulated, it forms a homodimer with Bcl2, binds to the channel on the mitochondrial membrane to increase its permeability, increases the release of Cyt C and promotes apoptosis (Zhang *et al.*, 2019). In addition, caspase-3 and caspase-9 are key enzymes in the caspase family. Caspase-9 is a promoter in the apoptotic pathway, which enters the Cyt C in the cytoplasm to form a complex to initiate the apoptotic process and then activates the proteolytic enzyme caspase-9, which undergoes self-cleavage to form Cleaved caspase-9 and the cleavage of caspase-9 further activates the proteolytic enzyme caspase-3, initiates the caspase cascade reaction and triggers mitochondrial signaling pathway-related apoptosis (Guan *et al.*, 2022). Cleaved caspase-3 is an activated form of caspase-3, whose expression can reflect the degree of apoptosis (Rashidbaghan *et al.*, 2020).

Similar to the results of previous studies, in this study, CA can induce apoptosis of human nasopharyngeal carcinoma cells and liver cancer cells by activating caspase-9/3 (Chen *et al.*, 2020; Feng *et al*., 2018). The results of this study also showed that CA could induce apoptosis of CRC cells and trigger cell cycle arrest. In summary, CA could inhibit the malignant progression of CRC and antagonize CRC.

Abnormal metabolism is associated with the occurrence of many tumors and AEG is considered to be one of the significant characteristics of tumors. The cell metabolism of glycolysis usually shows the characteristics of raised glucose uptake and lactic acid production. Therefore, glucose uptake level and lactic acid content can be used as effective indicators to reflect the level of glycolysis. The increase of lactic acid promotes the production of acidic and hypoxic microenvironment, induces the decomposition of extracellular matrix and promotes tumor invasion and metastasis (Sutendra and Michelakis, 2013).

The expression levels of metabolic enzymes and transporters related to the AEG pathway are significantly increased in CRC and these changes may be associated with the regulation of multiple signaling pathways and transcription factors (Zhan *et al.*, 2023). Transporters are highly expressed in a variety of cancer tissues and specific transporters and key enzymes are important participants in the AEG pathway and metabolism of CRC cells. Glucose metabolism is mediated with GLUT. GLUT1 is responsible for the input of glucose from the outside of the cell and plays an initial role in AEG. GLUT1 and GLUT3 have been shown to be membrane transporters that accelerate metabolism in current studies and their levels are associated with the high recurrence rate and low survival rate of CRC (Ancey *et al.*, 2018).

There are four isozymes of HK1, HK2, HK3 and HK4 in mammals. After binding to the outer membrane of mitochondria, HK1 and HK2 interact with each other through voltage-dependent anion channels, close to ATP, thus promoting AEG (Guo *et al.*, 2022). KATAGIRI M *et al*. (Katagiri *et al.*, 2017) found that HK2 is key for the AEG pathway of tumors. HK2 mediates the Warburg effect and promotes cell growth and invasion in CRC. In addition, HK2 status is significantly correlated with the poor prognosis of patients. HK2 is a crucial indicator for the prognosis evaluation of CRC and it is also one of the potential therapeutic targets, which provides a new idea for the treatment of CRC.

LDH is the last key enzyme in the conversion of pyruvate to lactic acid in the AEG pathway. It is composed of subunit lactate dehydrogenase A/B (LDHA/B) and has five different isomers. The study found that (Kocianova *et al.*, 2022), in cancer cells with active AEG pathway (including lymphoma, digestive system and reproductive system tumors), the expression of LDHA increased. After the expression increased, the tumor cells could obtain an invasive phenotype, which was highlighted by cell remodeling, angiogenesis and increased invasion and migration. In addition, increased LDHA activity is associated with tumor chemoradiation resistance. In summary, these key enzymes and proteins ensure the supply and transport of raw materials in the AEG pathway of CRC cells and ensure the smooth progress of glucose uptake, decomposition and lactate excretion.

As an efficient ectopic activator, PFKFB3 significantly enhances the activity of phosphofructokinase-1 (PFK-1). PFKFB3 is expressed in almost all cells that require glucose metabolism and is highly expressed in rapidly growing tissues. The expression of PFKFB3 is significantly up-regulated during mitosis in solid tumors and non-solid tumors and is also highly expressed in cells during hypoxia, inflammatory stimulation and DNA synthesis (Shi *et al.*, 2017). PFKFB3 is also believed to enhance glycolysis and promote the growth and movement of tumor cells. PFKFB3 is associated with tumorigenesis and may regulate the proliferation of tumor cells through RAS, mTOR and other pathways (Kotowski *et al.*, 2021).

Previous studies have shown that enhanced glycolysis and the expression levels of related enzymes (GLUT1, HK2 and PFKP) can promote CRC progression (Guan *et al.*, 2023). This study showed that CA could inhibit CRC progression by inhibiting AEG. In addition, this study also overexpressed PFKFB3 to verify this conclusion. After PFKFB3 overexpressed, the growth, movement and invasion ability of cells were obviously increased, the apoptosis rates were markedly decreased, so promoting glycolysis promoted the malignant progression of CRC. This again showed that CA inhibited AEG and thus inhibited the malignant progression of CRC.

PI3K/Akt pathway can not only affect the development and differentiation of normal cells, but also activate many downstream effector molecules, affecting the apoptosis, transcription, translation and metabolism of tumor cells. Akt is a vital downstream target kinase of the PI3K pathway. It is an anti-apoptotic signal molecule. When its expression is inhibited, it can weaken the activation of MDM2. MDM2 can bind to P53 and inhibit P53 transcriptional activity (Huang *et al.*, 2018) and P53 is an important tumor suppressor factor, which inhibits the proliferation of tumor cells and induces apoptosis. Evodiamine activates the PI3K/Akt/P53 pathway to inhibit CRC growth (Zheng *et al.*, 2024).

In addition, PI3K activation promotes Akt phosphorylation. Phosphorylated Akt can lead to phosphorylation of PFKFB2. Phosphorylation of PFKFB2 can increase the production of fructose 2,6-phosphate, which in turn promotes PFK1 activation. PFK1 is a key rate-limiting enzyme in glycolysis, resulting in increased glycolysis (Lee *et al.*, 2018).

Consistent with the previous results (Zheng *et al*., 2024), this study also found that the levels of p-PI3K and p-Akt proteins of SW480 and HT29 cells were markedly declined after CA intervention and the level of P53 protein was notably raised, suggesting that CA regulated PI3K/Akt/P53 axis. In addition, this conclusion was also verified by molecular docking. The results showed that CA could bind to AKT1 and TP53 stably. After the application of 740 Y-P, the AEG level of CRC cells increased significantly. In

conclusion, CA inhibited AEG in CRC cells via regulating the PI3K/Akt/P53 axis.

Finally, nude mice experiments again confirmed that CA inhibited AEG through PI3K/Akt/P53 axis, thereby inhibiting the malignant progression of CRC. However, this study has only been verified in a few CRC cells and transplanted tumors, lacking more experimental data of CRC cells and has not been combined with clinical practice, lacking relevant clinical verification. Whether the role of CA in the human body is also affected by PI3K/Akt/P53 pathway and glycolysis needs further research and demonstration. In order to better complete the clinical transformation, this study needs to further clarify the anti-tumor effect of CA through more CRC cell models and animal experiments and formulate a detailed clinical trial plan based on the experimental results. In addition, the safety and efficacy of CA also need to be further verified in future clinical trials. In addition, AEG is closely related to drug resistance, immune escape and metastasis of tumor cells. In the future, we will further study the effect of CA on drug resistance and immune microenvironment after inhibiting AEG of CRC cells, hoping to provide some theoretical basis and new ideas for clinical CRC treatment and new drug development.

CONCLUSION

In summary, this study confirmed that CA can inhibit AEG and adverse progression of CRC and its mechanism is achieved through regulating the PI3K/Akt/P53 pathway. This research offers an experimental basis for the treatment of CRC and CA provides a new perspective for the study of potential treatment strategies for CRC.

Consent to publish

The manuscript has neither been previously published nor is under consideration by any other journal. The authors have all approved the content of the paper.

Ethical approval

This study was approved by Nanyang Medical College Ethics Committee (No. 2025-0011, date: 2025.1.17).

Funding

1. Prediction of Molecular Targets and Construction of Prognostic Model for Compound Cantharidin Capsules in the Treatment of Colorectal Cancer (No. 23JCQY2036)
2. Development and application of a prognostic assessment model for esophageal squamous cell carcinoma related to estrogen metabolism genes (No. 232102310137).

Author contribution

[Yan Wei, Shulin Dai]: Developed and planned the study, performed experiments and interpreted results. Edited and refined the manuscript with a focus on critical intellectual contributions.

[Dongyun Zhang, Ting Zhang, Xiaoyu Wang, Bolin Liu, Wei Huang]: Participated in collecting, assessing and interpreting the date. Made significant contributions to date interpretation and manuscript preparation.

[Yin Li, Mingliao Niu]: Provided substantial intellectual input during the drafting and revision of the manuscript.

Conflicts of interest

The authors declare that they have no financial conflicts of interest.

REFERENCES

Abedizadeh R, Majidi F, Khorasani HR, Abedi H and Sabour D (2024). Colorectal cancer: A comprehensive review of carcinogenesis, diagnosis and novel strategies for classified treatments. *Cancer Metastasis Rev.,* **43**(2): 729-753.

Ancey PB, Contat C and Meylan E (2018). Glucose transporters in cancer - from tumor cells to the tumor microenvironment. *Febs. J.,* **285**(16): 2926-2943.

Bausys A, Kryzauskas M, Abeciunas V, Degutyte AE, Bausys R, Strupas K and Poskus T (2022). Prehabilitation in modern colorectal cancer surgery: A comprehensive review. *Cancers (Basel),* **14**(20): 5017.

Chen YC, Chen PN, Lin CW, Yang WE, Ho YT, Yang SF and Chuang CY (2020). Cantharidic acid induces apoptosis in human nasopharyngeal carcinoma cells through p38-mediated upregulation of caspase activation. *Environ. Toxicol.,* **35**(5): 619-627.

Feng IC, Hsieh MJ, Chen PN, Hsieh YH, Ho HY, Yang SF and Yeh CB (2018). Cantharidic acid induces apoptosis through the p38 MAPK signaling pathway in human hepatocellular carcinoma. *Environ. Toxicol.,* **33**(3): 261-268.

Fukushi A, Kim HD, Chang YC and Kim CH (2022). Revisited metabolic control and reprogramming cancers by means of the warburg effect in tumor cells. *Int. J. Mol. Sci.,* **23**(17): 10037.

Glaviano A, Foo ASC, Lam HY, Yap KCH, Jacot W, Jones RH, Eng H, Nair MG, Makvandi P, Geoerger B, Kulke MH, Baird RD, Prabhu JS, Carbone D, Pecoraro C, Teh DBL, Sethi G, Cavalieri V, Lin KH, Javidi-Sharifi NR, Toska E, Davids MS, Brown JR, Diana P, Stebbing J, Fruman DA and Kumar AP (2023). PI3K/AKT/mTOR signaling transduction pathway and targeted therapies in cancer. *Mol. Cancer,* **22**(1): 138.

Guan HM, Li WQ, Liu J and Zhou JY (2022). LncRNA HIF1A-AS2 modulated by HPV16 E6 regulates apoptosis of cervical cancer cells via P53/caspase9/caspase3 axis. *Cell Signal,* **97**: 110390.

Guan Y, Yao W, Yu H, Feng Y, Zhao Y, Zhan X and Wang Y (2023). Chronic stress promotes colorectal cancer progression by enhancing glycolysis through β2-AR/CREB1 signal pathway. *Int. J. Biol. Sci.,* **19**(7): 2006-2019.

Guo D, Tong Y, Jiang X, Meng Y, Jiang H, Du L, Wu Q, Li S, Luo S, Li M, Xiao L, He H, He X, Yu Q, Fang J and Lu Z (2022). Aerobic glycolysis promotes tumor immune evasion by hexokinase2-mediated phosphorylation of IκBα. *Cell Metab,* **34**(9): 1312-1324.e1316.

Hou Y, Zhang X, Yao H, Hou L, Zhang Q, Tao E, Zhu X, Jiang S, Ren Y, Hong X, Lu S, Leng X, Xie Y, Gao Y, Liang Y, Zhong T, Long B, Fang JY and Meng X (2023). METTL14 modulates glycolysis to inhibit colorectal tumorigenesis in p53-wild-type cells. *EMBO Rep.,* **24**(4): e56325.

Huang Q, Chen L, Yang L, Xie X, Gan L, Cleveland JL and Chen J (2018). MDMX acidic domain inhibits p53 DNA binding in vivo and regulates tumorigenesis. *Proc. Natl. Acad. Sci. U S A,* **115**(15): E3368-e3377.

Icard P, Shulman S, Farhat D, Steyaert JM, Alifano M and Lincet H (2018). How the Warburg effect supports aggressiveness and drug resistance of cancer cells? *Drug Resist. Updat,* **38**: 1-11.

Katagiri M, Karasawa H, Takagi K, Nakayama S, Yabuuchi S, Fujishima F, Naitoh T, Watanabe M, Suzuki T, Unno M and Sasano H (2017). Hexokinase 2 in colorectal cancer: A potent prognostic factor associated with glycolysis, proliferation and migration. *Histol. Histopathol.,* **32**(4): 351-360.

Kocianova E, Piatrikova V and Golias T (2022). Revisiting the Warburg effect with focus on lactate. *Cancers (Basel),* **14**(24): 6028.

Kotowski K, Rosik J, Machaj F, Supplitt S, Wiczew D, Jabłońska K, Wiechec E, Ghavami S and Dzięgiel P (2021). Role of PFKFB3 and PFKFB4 in Cancer: Genetic basis, impact on disease development/progression and potential as therapeutic targets. *Cancers (Basel),* **13**(4): 909.

Lee JH, Liu R, Li J, Wang Y, Tan L, Li X J, Qian X, Zhang C, Xia Y, Xu D, Guo W, Ding Z, Du L, Zheng Y, Chen Q, Lorenzi P L, Mills G B, Jiang T and Lu Z (2018). EGFR-phosphorylated platelet isoform of phosphofructokinase 1 promotes PI3K activation. *Mol. Cell,* **70**(2): 197-210.e197.

Lin J, Xia L, Oyang L, Liang J, Tan S, Wu N, Yi P, Pan Q, Rao S, Han Y, Tang Y, Su M, Luo X, Yang Y, Chen X, Yang L, Zhou Y and Liao Q (2022). The POU2F1-ALDOA axis promotes the proliferation and chemoresistance of colon cancer cells by enhancing glycolysis and the pentose phosphate pathway activity. *Oncogene.,* **41**(7): 1024-1039.

Liu J, Zhang C, Hu W and Feng Z (2015). Tumor suppressor p53 and its mutants in cancer metabolism. *Cancer Lett,* **356**(2 Pt A): 197-203.

Liu M, Hu Y, Lu S, Lu M, Li J, Chang H, Jia H, Zhou M, Ren F and Zhong J (2020). IC261, a specific inhibitor of CK1δ/ε, promotes aerobic glycolysis through p53-dependent mechanisms in colon cancer. *Int. J. Biol. Sci.,* **16**(5): 882-892.

Lou F and Zhang M (2023). RFC2 promotes aerobic glycolysis and progression of colorectal cancer. *BMC Gastroenterol,* **23**(1): 353.

Pu H, Qian Q, Wang F, Gong M and Ge X (2021). Schizandrin A induces the apoptosis and suppresses the proliferation, invasion and migration of gastric cancer cells by activating endoplasmic reticulum stress. *Mol. Med. Rep.,* **24**(5): 787.

Qin R, Fan X, Huang Y, Chen S, Ding R, Yao Y, Wu R, Duan Y, Li X, Khan HU, Hu J and Wang H (2024). Role of glucose metabolic reprogramming in colorectal cancer progression and drug resistance. *Transl. Oncol.,* **50**: 102156.

Rashidbaghan A, Mostafaie A, Yazdani Y and Mansouri K (2020). Urtica dioica agglutinin (a plant lectin) has a caspase-dependent apoptosis induction effect on the acute lymphoblastic leukemia cell line. *Cell Mol. Biol. (Noisy-le-grand),* **66**(6): 121-126.

Shi L, Pan H, Liu Z, Xie J and Han W (2017). Roles of PFKFB3 in cancer. *Signal Transduct. Target. Ther.,* **2**: 17044.

Su D (2022). MCM7 affects the cisplatin resistance of liver cancer cells and the development of liver cancer by regulating the PI3K/Akt signaling pathway. *Immunopharmacol. Immunotoxicol.,* **44**(1): 17-27.

Sun Y, Zhang H, Meng J, Guo F, Ren D, Wu H and Jin X (2022). S-palmitoylation of PCSK9 induces sorafenib resistance in liver cancer by activating the PI3K/AKT pathway. *Cell Rep,* **40**(7): 111194.

Sutendra G and Michelakis ED (2013). Pyruvate dehydrogenase kinase as a novel therapeutic target in oncology. *Front. Oncol.,* **3**: 38.

Wang Q, Wang B, Zhang W, Zhang T, Liu Q, Jiao X, Ye J, Hao Y, Gao Q, Ma G, Hao C and Cui B (2024). APLN promotes the proliferation, migration and glycolysis of cervical cancer through the PI3K/AKT/mTOR pathway. *Arch. Biochem. Biophys.,* **755**: 109983.

Wang S, Cheng Z, Cui Y, Xu S, Luan Q, Jing S, Du B, Li X and Li Y (2023). PTPRH promotes the progression of non-small cell lung cancer via glycolysis mediated by the PI3K/AKT/mTOR signaling pathway. *J. Transl. Med.,* **21**(1): 819.

Wang SC, Chow JM, Chien MH, Lin CW, Chen HY, Hsiao PC and Yang SF (2018). Cantharidic acid induces apoptosis of human leukemic HL-60 cells via c-Jun N-terminal kinase-regulated caspase-8/-9/-3 activation pathway. *Environ. Toxicol.,* **33**(4): 514-522.

Xi Y, Garshott DM, Brownell AL, Yoo GH, Lin HS, Freeburg TL, Yoo NG, Kaufman RJ, Callaghan MU and Fribley AM (2015). Cantharidins induce ER stress and a terminal unfolded protein response in OSCC. *J. Dent. Res.,* **94**(2): 320-329.

Yan J, Gao YM, Deng XL, Wang HS and Shi GT (2023). Integrative analysis of the molecular signature of target genes involved in the antitumor effects of cantharidin on hepatocellular carcinoma. *BMC Cancer,* **23**(1): 1161.

Yang Z and Liu Z (2020). The efficacy of (18)F-FDG PET/CT-based diagnostic model in the diagnosis of colorectal cancer regional lymph node metastasis. *Saudi. J. Biol. Sci.,* **27**(3): 805-811.

Zhan L, Su F, Li Q, Wen Y, Wei F, He Z, Chen X, Yin X, Wang J, Cai Y, Gong Y, Chen Y, Ma X and Zeng J (2023). Phytochemicals targeting glycolysis in colorectal cancer therapy: Effects and mechanisms of action. *Front. Pharmacol.,* **14**: 1257450.

Zhang S, Yang Y, Hua Y, Hu C and Zhong Y (2020). NCTD elicits proapoptotic and antiglycolytic effects on colorectal cancer cells via modulation of Fam46c expression and inhibition of ERK1/2 signaling. *Mol. Med. Rep.,* **22**(2): 774-782.

Zhang Y, Yang X, Ge X and Zhang F (2019). Puerarin attenuates neurological deficits via Bcl-2/Bax/cleaved caspase-3 and Sirt3/SOD2 apoptotic pathways in subarachnoid hemorrhage mice. *Biomed. Pharmacother.,* **109**: 726-733.

Zheng Q, Jing S, Hu L and Meng X (2024). Evodiamine inhibits colorectal cancer growth via RTKs mediated PI3K/AKT/p53 signaling pathway. *J. Cancer,* **15**(8): 2361-2372.